SUPPLEMENTARY MATERIALS of

Discovering the 3' UTR-Mediated Regulation of Alpha-Synuclein

Domenica Marchese[1,2], Teresa Botta-Orfila[1,2], Davide Cirillo[1,2,3], Juan Antonio Rodriguez[2,4], Carmen Maria Livi[1,2,5], Rubén Fernández-Santiago[6,7], Mario Ezquerra[6,7], Maria J. Martí[6,7], Elias Bechara[1,2]
and Gian Gaetano Tartaglia[1,2,8,9 *]

[1] Centre for Genomic Regulation (CRG), The Barcelona Institute for Science and Technology, Dr. Aiguader 88, 08003 Barcelona, Spain
[2] Universitat Pompeu Fabra (UPF), Barcelona, Spain
[3] Barcelona Supercomputing Center (BSC), Torre Girona c/Jordi Girona, 29, 08034 Barcelona, Spain

[4] Centro Nacional de Análisis Genómico, c/BaldiriReixac, 4, 08028 Barcelona, Spain

[5] IFOM, the FIRC Institute of Molecular Oncology, Via Adamello 16, 20139 Milan, Italy

[6] Institut d'Investigacions Biomèdiques August Pi i Sunyer (IDIBAPS), Barcelona, Spain.

[7] Parkinson's Disease and Movement Disorders Unit, Institut de Neurociències Hospital Clínic, CIBERNED, Barcelona, Spain.

[8] Institucio Catalana de Recerca i Estudis Avançats (ICREA), Barcelona,Spain.

[9] on behalf of the Catalan MSA Registry (CMSAR) – Table 1.

*Corresponding author: Gian Gaetano Tartaglia

_cat_RAPID ranking analysis

The algorithm developed by our group, *cat*RAPID (1) was used to compute the interaction propensity of *SNCA* long 3'UTR with candidate proteins identified by protein arrays. *cat*RAPID *omics* (2) ranks protein-RNA pairs based on the interactions score, presence of specific RNA motifs and RNA-binding domains. For RNA sequences > 1000 nt, the uniform fragmentation procedure is applied to determine the binding regions of a protein. Protein interactions were sorted by the median value of *cat*RAPID *omics* ranking score (2) (**Fig. 1D**). We used *cat*RAPID *Global Score* (3) to compute the interaction propensity of each RBP by integrating the interaction propensities over RNA fragments. Both the fragment scores and *Global Score* significantly discriminate interacting vs non-interacting pairs (**Supp. Fig. 1**).

RNA 3'end sequencing

SH-SY5Y cells were *in vitro* differentiated towards a dopaminergic neuron-like phenotype by treatment with retinoic acid (RA), during four days, and 12-O-tetradecanoyl-phorbol-13-acetate (TPA), during three days. Total RNA was isolated from HeLa and *in vitro* differentiated SH-SY5Y cells with RNeasy Mini kit (Qiagen) and used for the first strand cDNA synthesis with OligodT carrying a 5' flanking region containing the sequence of the Unique Molecular Identifier (UMI) and the R2 sequencing adaptor. A first PCR amplification was performed with a pool of forward PCR specific primers annealing to different regions of the 3'UTR and carrying 5' flanking regions containing the R1 sequencing adaptor, and the Index primer, annealing to the R2 adaptor. This was followed by a second PCR amplification with Universal PCR primer and TS Oligo 2. After purification with AMPure WP Beads, the quality of the library was assessed on an Agilent Bioanalyzer DNA 1000 Chip. DNA libraries were subjected to 50 bases pair end sequencing.

RNA 3'end sequencing data analysis

The unique molecular identifier (UMI) was transferred from the second read pair to the first one's header and the left pair read was mapped to the gene of interest. The UMI in the header was used to check PCR duplicates and to group together reads with multiple mapping. In that case only the read with the largest coordinate was counted. Every mapping smaller than 25 nt was removed and a tolerance of +8 bases for reads count was admitted to avoid PCR artifacts. The ratio on the total number of reads mapping to those intervals was calculated.

RNA affinity purification

33 moles of biotinylated RNA were bound to Streptavidin magnetic beads (Dynabeads M-280, Invitrogen) previously blocked with 100 ng/ul of tRNAs in NT2 buffer (50 mM Tris-HCl pH 7.5, 150 mM NaCl, 1 mM $MgCl_2$, 0.05% NP-40, 1 mM DTT). 2 mg of SH-SY5Y total cell extracts were added and incubated for 1 hour at room temperature, in presence of 1X Protease Inhibitors cocktails (Sigma Aldrich), 320 ng/ul Heparin (Sigma Aldrich), 4.3 ug/ul of Creatine Phosphate and 80 ng/ul of Creatine Kinase. Samples were cross-linked with 6000x100 uJ/cm^2 of energy and 254 nm UV light. Beads with RNA-protein complexes were washed two times with buffers NT2, HSB300, HSB500, HSB1000 with increasing salt

concentration. Bound proteins were eluted by RNase cocktail digestion in elution buffer (10 mM Tris-HCl pH 7.2, 1 mM MgCl2, 40 mM NaCl). Eluted proteins from 3'UTRS RNA, 3'UTRL RNA and negative control samples were analyzed by western blot for the detection of ELAVL1, TIAR and FMR1 negative control.

The RNA affinity purification was done in technical triplicates and the western blot was quantified using ImageJ analysis software. Statistical significance of binding differences, were determined by a Student's T-test

RNA electrophoretic mobility shift assay

5 fmoles of probe were incubated with increasing concentrations of GST-TIAR or GST-ELAVL1 proteins (0, 100, 200 and 500 nM) in 1 X binding buffer (10 mM Tris-HCl, 150 mM NaCl, 0.1 mM DTT, 0.1 mM EDTA, 0.01% NP-40, 1% glycerol, 500 µg/ml yeast tRNAs). Samples were UV cross-linked and ran in a 4% acrylamide gel. After drying for 30 min the gel was exposed to a phosphor screen (GE Healthcare) during adequate time (~1 hour) and the radioactivity signal was detected by a Typhoon Trio instrument (GE Amersham).

For the competition assay 5 fmoles of radiolabeled probe were incubated with increasing concentrations of the non-labeled probes for A, B or C fragments (0.1 nM, 1 nM and 10 nM final concentration) during 10 minutes at room temperature. TIAR or ELAVL1 proteins were added at the dissociation constant concentration (200 nM for TIAR and 100 nM for ELAVL1) in 1X binding buffer and incubated for 15 minutes at room temperature. Samples were cross-linked and analyzed on a 4% acrylamide gel as described above. For 100, 200 and 500 nM of TIAR and ELAVL1, we measured the following protein:RNA ratios 30:1, 60:1 and 150:1 for fragment A, 38:1, 76:1 and 190:1 for fragment B, and 45:1, 90:1 and 225:1 for fragment C).

TIAR and ELAVL1 knockdown

HeLa cells (courtesy of Luciano Di Croce's lab) were cultured under standard conditions. TIAR and ELAVL1 short hairpin RNA (shRNA) constructs were generated by annealing single stranded complementary oligonucleotides (Sigma Aldrich) and cloned in pLKO.1 TRC-puro plasmid digested with AgeI and EcoRI.

60% confluent Hek293T cells were transfected with pLKO-shRNA (TIAR shRNA, ELAVL1 shRNA), or pLKO-empty vector (negative control), pCMV-VSV-G and pCMVDR-8.91 plasmids, to produce pLKO-shRNA-containing lentivirus. Medium containing lentivirus was collected after 40 and 48 h, filtered, supplemented with 5 µg/ml polybrene (Sigma Aldrich) and used to infect HeLa cells. Infected cells were selected with 2.5 µg/ml puromycin (Sigma Aldrich) and the efficacy of the knockdown was checked 24 h after selection by real-time PCR and western blot. Samples collected 3 days after selection were used to check the expression of α-synuclein at the mRNA and protein level.

RNA isolation and RT-qPCR were performed as described above and relative expression levels were calculated with the ΔΔCq method, using GAPDH as well as ACTB, PP1B and RPS18 and as reference genes. Average values of biological replicates were calculated and Wilcoxon's test was performed to assess for significant differences in gene expression between knockdown and control cells.

Proteins were extracted by lysing the cells with Pierce lysis buffer (Thermo Fisher Scientific) supplemented with Protease and Phosphatase Inhibitors (Thermo Fisher Scientific). Samples were analyzed by western blot using following antibodies: ab93432 (Abcam) for human α-synuclein, ab54987 (Abcam) for ELAVL1, sc-1749 (Santa Cruz) for TIAR and ab7291 (Abcam) for β-tubulin, which was used as internal reference protein for normalization with ImageJ (12).

TIAR and ELAVL1 overexpression

HeLa cells at 80-90% of confluency were transfected with pCMV-AC-ELAVL1 (OriGene Technologies) for ELAVL1 overexpression or pEGFP_G-TIAR (Clontech, courtesy of Valcarcel's Lab) for TIAR overexpression, using Lipofectamine 2000 according to manufacturer's instructions. pcDNA3.1-EGFP was used as a control plasmid for both overexpression experiments. Cells were collected 48 h after transfection and *SNCA* mRNA and protein levels were checked by real-time PCR and western blot (see above). The mean values of technical triplicates were calculated.

High throughput microRNAs expression analysis

We tested the level of expression of microRNAs in HeLa using a high throughput miRNAs expression analysis. In this approach, we hybridized total RNA extracted with miRNeasy kit (Qiagen) on a GeneChip miRNA 4.0 array (Thermo Fisher Scientific) that was analyzed with the Transcriptome Analysis Console (TAC) software (Thermo Fisher Scientific).

We obtained a list of 4628 microRNAs with a fluorescence signal in the range 0.56 - 14.1 ($\log_2$ scale) following a gamma distribution (shape parameter = 2.15; scale parameter = 1.07; fitting correlation >0.90). Around 10% of all microRNAs (432 cases) had a fluorescence signal >5, which is associated with good detectability (>1 standard deviation from the mean). Indeed, accurate quantification of expression levels has been previously achieved for cancer microRNAs (7) with fluorescence signals >5 in HeLa micro-arrays (including miR-776-36, miR-21-5-p, miR-378a-3p, miR-3156-5p, miR-181a-5p, miR-125a-5p and miR-320a with respective intensities of 5.82, 8.04, 9.89, 10.52, 10.53 11.40 and 13.34 in our assay). Among the microRNAs overlapping with TIAR and ELAVL1 binding sites we found hsa-miR-1224-5p and hsa-miR-3065-5p (non-conserved) whose expression levels are below the threshold (intensities: values 4.0 and 3.5), indicating poor expression in HeLa cells. In accordance with this result, an external dataset taken from a published high throughput small RNA sequencing analysis (8) reveals nearly undetectable levels of expression of microRNAs overlapping with TIAR and ELAV1 binding sites **(Suppl. Table 3)**.

Overall, our analysis indicates that microRNAs levels of expression are poor in two independent HeLa cell lines, as also directly observed for miR-7 (micro-array intensity: 2.71) and miR-153 (micro-array intensity: 1.34) by TaqMan assay. We ruled out that these miRNAs might have any relevant role in TIAR and ELAVL1 dependent SNCA regulation in the cell model used for our functional assays.

Measurement of luciferase mRNA levels

RNA was purified with *RNeasy* Mini kit and reverse transcribed with SuperScript III First-Strand synthesis SuperMix for qRT-PCR (Invitrogen). Real-time PCR was performed with 10 ng of cDNA template, 250 uM forward and reverse primers and 1X Sybr Green PCR master mix (Applied biosystem). The mRNA of *Renilla* luciferase was used to normalize *Firefly* luciferase mRNA levels.

Polysome Profiling

HeLa control, TIAR and ELAVL1 knockdown cells were grown under standard conditions. Incubation with the translation inhibitor cycloheximide (100 µg/ml) was performed at 70% cell confluence, for 15 min at 37°C. Cells were washed with cold 1X PBS and lysed on ice with Polysome lysis buffer (10 mM Tris-HCl pH 7.4, 100 mM KCl, 10 mM $MgCl_2$, 1% Triton-X 100, 2.5 U/ml Turbo DNase, 2 mM DTT, 1X protease inhibitors, 100 µg/ml cycloheximide, 200 U/ml Superase In).

Lysates from three 10 cm^2 dishes were transferred to a tube containing 425-600 microns glass beads (Sigma). After vortex and centrifugation for 5 min at 5000 g at 4°C, lysates were transferred to new tubes and immediately snap-frozen in liquid nitrogen. 9-12 OD_{260} were loaded onto a 10-50% sucrose gradient in a Beckman SW 41Ti rotor and subjected to ultracentrifugation for 150 min at 35000 g at 4°C using a Beckman Optima XL-100 K centrifuge. The gradients were fractioned by upward displacement using a gradient fractionator connected to a BioRad Econo UV monitor, peristaltic pump, and fraction collector. 5 ng of *in vitro* synthesized *firefly* luciferase RNA were added to each fraction as an internal control for RNA precipitation efficiency. Samples were precipitated overnight at -20°C with 100% ethanol and then the pellets were washed with 80% ethanol and resuspended before isolating RNA using Maxwell 16 LEV simply RNA cells kit (Promega).

A fixed volume of RNA was used for reverse transcription and real-time PCR (see above). In order to have a standard curve-based relative quantification, we used serial dilutions of a cDNA sample to which we assigned arbitrary values for each of the genes of interest (e.g. 100 AU to 12.5 ng, 10 AU to 1.25 ng, 1 AU to 0.125 ng, etc.). The values of *SNCA* for each polysomal fraction (x_1, x_2, …x_{16}) obtained by interpolation with the standard curve, were then normalized to the Firefly luciferase signal, which was used as internal control RNA to correct for differences in RNA precipitation efficiencies.

The total amount of *SNCA* in all fractions was calculated as the sum of the corrected values. The ratio ($x_{n=1-16}/\sum x_n$) against the total for each fraction was calculated and represented as percentage of *SNCA* mRNA in each polysomal fraction. The average and standard deviation of biological triplicates were calculated for each condition (control, TIAR kd and ELAVL1

kd) and the results were compared. ACTB was used as a negative control since its distribution along the polysomal fractions is not affected by TIAR or ELAVL1 knockdown.

trans-eQTLs analysis

For trans eQTLs analysis, we selected a comprehensive genomic region including *TIAR-INPP5F* genes plus ~84 kb upstream *TIAR* and ~94 kb downstream *INPP5F*. The vcf files containing SNP data for the region chr10:121250246-121682830 (hg19) were downloaded from the 1000 Genomes Project (4). After filtering the region for variants only present in European ancestry individuals (CEU population; n=85) with an allele frequency of at least 5%, we calculated trans-eQTLs in relation to *SNCA* in all available brain-related tissues in GTEx, namely: anterior cingulate cortex, caudate basal ganglia, cerebellar hemisphere, cerebellum, brain cortex, frontal cortex, hippocampus, hypothalamus, nucleus accumbens basal ganglia and putamen basal ganglia. We therefore generated p-values of trans-eQTL association for *SNCA* for all the 892 SNPs for every tissue (taking into account that data were not always available for all 892 SNPs in all tissues).

To test the likelihood of obtaining such p-values for *SNCA* trans eQTLs ($9e^{-5}$), we selected 100 random genes from the protein array not interacting genes. These genes were matched by length with *TIAR* (+/- 15 kb). Next, we identified the corresponding SNP variants, keeping again only variants with a 5% allele frequency in CEU population, To avoid testing redundant information, linkage disequilibrium (LD) blocks within this dataset were estimated by PLINK's pruning algorithm (5) with an $R^2 > 0.8$ and using a sliding window of 50 SNPs, moving it 5 SNPs per iteration and using CEU individuals as reference. The average number of LD blocks (or tag-SNPs per gene) was 34 (s.d=19). *TIAR* contains 38 tag-SNPs, falling in percentile 67 of the distribution. This confirms that *TIAR* is comparable within our random sample. All 22,818 selected tag-SNPs for the 100 random genes were tested for being trans-eQTLs for *SNCA* in 10 brain tissues in GTEx project. A total sum of 223 independent tag-SNPs for the ten tissues were tested regarding *TIAR*. The random sample of tag-SNPs (n=22,818) returned only 3 SNPs reaching TIAR SNP highest p-value ($9e^{-5}$). A binomial test was applied to show that our results are unlikely to be observed by chance (binomial test pvalue = 0.02).

GWAS analysis

GWAS p-values for *TIAR* region were downloaded from the PDgene web (http://www.pdgene.org/view?gene=TIAL1), which reports p-values from the GWAS meta-analysis by Nalls et al. (6). PLINK (5) was used to test whether our significant *SNCA* trans eQTLs in TIAR region presented LD with the top significant SNPs associated to PD.

Appendix

Primer for SNCA 3'UTR cloning in pBSK plasmid

ApaI-Syn3UTR Fw
CGGGGCCCGGAAATATCTTTGCTCCCAGT

NotI-Syn3UTRS Rv GCGCGGCCGCgTATTTTTGCAATGAGATAACGT

NotI-Syn3UTRL Rv GCGCGGCCGCGTATTTTCATATATGTATATATT

BamHI-Syn3UTRM Rv
CGGGATCCCATGGTCGAATATTATTTATTG

Syn3UTRL flanking Fw GAAGGGTATCAAGACTACGAACCTGAAGCC

Syn3UTRL flanking Rv GAACAAGGGTTTTAGGAGCTCTTTGTAAG

Primers for construct sequencing

T7 promoter TAATACGACTCACTATAGGG
T3 promoter GCAATTAACCCTCACTAAAGG
SYN3UTRLseq1 ACTGTTGTTTGATGTGTATG
Syn3UTRLseq2GCCTAGAATTCATATATTTGGC
Syn3UTRLseq3CCTAGAATTCATATATTTGGC

Primers for real-time PCR

SNCA Fw AGGGTGTTCTCTATGTAGG
SNCA Rv ACTGTCTTCTGGGCTACTGC

TIAR Fw GCCAATGGAGCCAAGTGTAT
TIAR Rv CATATCCGGCTTGGTTAGGA

ELAVL1 Fw AAAACCATTAAGGTGTCGTATGCTC
ELAVL1 Rv CCTCTGGACAAACCTGTAGTCTGAT

GAPDH Fw GACCACAGTCCATGCCATC
GAPDH Rv TTCAGCTCAGGGATGACCTT

ACTB Fw GGACCTGACTGACTACCTCAT
ACTB rv CGTAGCACAGCTTCTCCTTAAT

Primers for Gibson cloning

pGL4-TK-FL linearization

pGL4-TK-FL Fw

CTTCGAGCAGACATGATAAGATACATTGATGAGTTT
pGL4-TK-FL Rv
TTATTACACGGCGATCTTGCCGC

3'UTRs amplification from pBSK plasmid

All_3UTRs_Gibs Fw
GCAAGATCGCCGTGTAATAAGAAATATCTTTGCTCCCAGT
3UTRS-Gibs Rv
CTTATCATGTCTGCTCGAAGTCCACCGTATTTTTGCAATGAGATAACGT
3UTRM-Gibs Rv
TTATCATGTCTGCTCGAAGCGGCGTGCATGGTCGAATATTATTTATTG
3UTRL-Gibs Rv
CTTATCATGTCTGCTCGAAGTATTTTCATATATGTATATATT

Primers/Gibson oligos for PAS deletion

Δ(262-267) Fw AACACCTAAGTGACTACCACTTATTTCTAAATC
Δ(262-267) Rv TTGTTTTAACATCGTAGATTGAAGCC

Δ(262-267)Gibson oligos
Fw: GCTTCAATCTACGATGTTAAAACAAAACACCTAAGTGACTACCACTTATT
Rv: AATAAGTGGTAGTCACTTAGGTGTTTTGTTTTAACATCGTAGATTGAAGC

Δ(468-473)Fw TACTAAATATGAAATTTTACCATTTTGCG
Δ(468-473)Rv GGTGCATAGTTTCATGCTCACAT

Δ(468-473)Gibson oligos
Fw: ATATGTGAGCATGAAACTATGCACCTACTAAATATGAAATTTTACCATTT
Rv: AAATGGTAAAATTTCATATTTAGTAGGTGCATAGTTTCATGCTCACATAT

Δ(529-553)Fw ACGTTATCTCATTGCAAAAATATT
Δ(529-553)Rv TACAAACACAAGTGAATAAAACACA

Δ(529-553)Gibson oligos
Fw: TGTGTTTTATTCACTTGTGTTTGTAACGTTATCTCATTGCAAAAATATTT
Rv: AAATATTTTTGCAATGAGATAACGTTACAAACACAAGTGAATAAAACACA

Δ(1054-1059)Fw TAATATTCGACCATGAATAAAA
Δ(1054-1059)Rv GTCAGAAAGGTACAGCATTCAC
Δ(1054-1059)Fw TAATATTCGACCATGCACGCCG (for 3UTRM)

Δ(1054-1059)Gibson oligos
Fw: GGTGTGAATGCTGTACCTTTCTGACTAATATTCGACCATGAATAAAAAAA
Rv: TTTTTTTATTCATGGTCGAATATTAGTCAGAAAGGTACAGCATTCACACC

Primers for real-time PCR of luciferase assay

Luc FW: ACCTTCGTGACTTCCCATTT
Luc RV: GGTACTGCCACTACTGTTCAT

Ren FW: TTGAATCATGGGATGAATGG
Ren RV: ATGTTGGACGACGAACTTCA

Luc-3UTRS FW: TGTGAGCATGAAACTATGCACCT
Luc-3UTRS RV: TCATGTCTGCTCGAAGTCCACC

Luc-3UTRM FW: TGGGGAACTGTTGTTTGATGTGT
Luc-3UTRM RV: CGGCGTGCATGGTCGAATATTA

Luc-3UTRL FW GTGAATGCTGTACCTTTCTGACTAAT
Luc-3UTRL RV CAGAGCCTTGAATGTGCTAATATGT

Short hairpin RNAs for knockdown

shTIAR forward oligo:
CCGGCCCATATTGCTTTGTGGAATTCTCGAGAATTCCACAAAGCAATATGGGTTT
TTG

shTIAR reverse oligo:
AATTCAAAAACCCATATTGCTTTGTGGAATTCTCGAGAATTCCACAAAGCAATAT
GGGT

shELAVL1 forward oligo:
CCGGTACCAGTTTCAATGGTCATAACTCGAGTTATGACCATTGAAACTGGTATTTT
TG

shELAVL1 reverse oligo:
AATTCAAAAATACCAGTTTCAATGGTCATAACTCGAGTTATGACCATTGAAACTG
GTA

shTIAR forward oligo 2:

CCGGATTCATGATAGGCTTCGATTTCTCGAGAAATCGAAGCCTATCATGAATTTTT
TG

shTIAR reverse oligo 2:

CAAAAAATTCATGATAGGCTTCGATTTCTCGAGAAATCGAAGCCTATCATGAATC
CGG

shELAVL1 forward oligo 2:
CCGGCGAGCTCAGAGGTGATCAAAGCTCGAGCTTTGATCACCTCTGAGCTCGTTT
TTG

shELAVL1 reverse oligo 2:
CAAAAACGAGCTCAGAGGTGATCAAAGCTCGAGCTTTGATCACCTCTGAGCTCGC
CGG

Primers for 3'end RNA sequencing

R1-SNC608
CCCTACACGACGCTCTTCCGATCTtatgcctgtggatcctgaca
R1-SNC909
CCCTACACGACGCTCTTCCGATCTctgtggattttgtggcttca
R1-SNC1154
CCCTACACGACGCTCTTCCGATCTtgagcatgaaactatgcacct
R1-SNC1432
CCCTACACGACGCTCTTCCGATCTctgaagcaacactgccagaa
R1-SNC1713
CCCTACACGACGCTCTTCCGATCTttggtgtgaatgctgtaccttt
R1-SNC2004
CCCTACACGACGCTCTTCCGATCTtgcctttaaacatcgttgga
R1-SNC2353
CCCTACACGACGCTCTTCCGATCTatatattgggcgctggtgag
R1-SNC2787
CCCTACACGACGCTCTTCCGATCTtgacggtaatttttgagcagtg
R1-SNC3013
CCCTACACGACGCTCTTCCGATCTggtcggctttaccaaaacag

R2-UMI-dT16
VNTTCAGACGTGTGCTCTTCCGATCTNNNNNNNNNNTTTTTTTTTTTTTTTTVN

Antibodies

Rabbit polyclonal anti-alpha Synuclein antibody [ab93432]
Mouse monoclonal anti-HuR/ELAVL1 [ab54987]
Goat polyclonal anti-TIAR [sc-1749]
Rabbit polyclonal anti-FMRP [ab69815]
Mouse monoclonal anti-alpha Tubulin antibody [ab7291]

Protein G HRP-conjugate (Millipore, 18-161)
Rabbit polyclonal secondary antibody to Mouse IgG-HRP [ab97046]

1. Bellucci,M., Agostini,F., Masin,M. and Tartaglia,G.G. (2011) Predicting protein associations with long noncoding RNAs. *Nat. Methods*, **8**, 444–445.

2. Agostini,F., Zanzoni,A., Klus,P., Marchese,D., Cirillo,D. and Tartaglia,G.G. (2013) catRAPID omics: a web server for large-scale prediction of protein-RNA interactions. *Bioinformatics*, 10.1093/bioinformatics/btt495.

3. Cirillo,D., Blanco,M., Armaos,A., Buness,A., Avner,P., Guttman,M., Cerase,A. and Tartaglia,G.G. (2016) Quantitative predictions of protein interactions with long noncoding RNAs. *Nat. Methods*, **14**, 5–6.

4. 1000 Genomes Project Consortium, Auton,A., Brooks,L.D., Durbin,R.M., Garrison,E.P., Kang,H.M., Korbel,J.O., Marchini,J.L., McCarthy,S., McVean,G.A., *et al.* (2015) A global reference for human genetic variation. *Nature*, **526**, 68–74.

5. Purcell,S., Neale,B., Todd-Brown,K., Thomas,L., Ferreira,M.A.R., Bender,D., Maller,J., Sklar,P., de Bakker,P.I.W., Daly,M.J., *et al.* (2007) PLINK: a tool set for whole-genome association and population-based linkage analyses. *Am. J. Hum. Genet.*, **81**, 559–575.

6. Nalls,M.A., Pankratz,N., Lill,C.M., Do,C.B., Hernandez,D.G., Saad,M., DeStefano,A.L., Kara,E., Bras,J., Sharma,M., *et al.* (2014) Large-scale meta-analysis of genome-wide association data identifies six new risk loci for Parkinson's disease. *Nat. Genet.*, **46**, 989–993.

7. Ferracin,M., Lupini,L., Salamon,I., Saccenti,E., Zanzi,M.V., Rocchi,A., Da Ros,L., Zagatti,B., Musa,G., Bassi,C., *et al.* (2015) Absolute quantification of cell-free microRNAs in cancer patients. *Oncotarget*, **6**, 14545–14555.

8. Grolmusz,V.K., Tóth,E.A., Baghy,K., Likó,I., Darvasi,O., Kovalszky,I., Matkó,J., Rácz,K. and Patócs,A. (2016) Fluorescence activated cell sorting followed by small RNA sequencing reveals stable microRNA expression during cell cycle progression. *BMC Genomics*, **17**, 412.

9. Dassi,E., Malossini,A., Re,A., Mazza,T., Tebaldi,T., Caputi,L. and Quattrone,A. (2012) AURA: Atlas of UTR Regulatory Activity. *Bioinforma. Oxf. Engl.*, **28**, 142–144.

10. Dassi,E., Re,A., Leo,S., Tebaldi,T., Pasini,L., Peroni,D. and Quattrone,A. (2014) AURA 2: Empowering discovery of post-transcriptional networks. *Transl. Austin Tex*, **2**, e27738.

SUPPLEMENTARY TABLES

Supp. Table 1. List of control individuals, PD and MSA cases used for analysis of protein levels in motor cortex post-mortem biopsies. Abbreviations: ARP=Alzheimer's disease related pathology (NFT: neurofibrillary tangles I-VI according to Braak, amyloid plaques A-C according to CERAD); iLBD: incidental Lewy-body disease; SVD: small vessel disease, AgD: argyrophilic grain pathology; OPCA, Olivopontocerebellar atrophy; SND, striatonigral degeneration; PD-D: Parkinson's disease with dementia; n.a.: not available; PMD: postmortem delay.

Supp. Table 2. List of control individuals, PD and MSA cases used for analysis of protein levels in primary fibroblasts obtained from skin biopsies. Abbreviations: AAO: Age at onset; MSA-P: Multiple System Atrophy-parkinsonian type; sPD: sporadic Parkinson's Disease; L2PD: LRRK2-associated Parkinson's Disease, n.a.: not available.

Supp. Table 3. miRNAs overlapping TIAR and ELAVL1 binding sites (coordinates relative to the 3' UTR). In accordance with our results, an external dataset taken from a published high throughput small RNA sequencing analysis reveals undetectable expression levels of TIAR/ELAV1 overlapping miRNAs in HeLa cells (8).

Supp. Table 4. We identified 67 SNPs: 5 SNPs fall into ELAVL1 binding sites, 3 in TIAR binding sites and 2 are located in ELAVL1/TIAR shared binding regions. 6 of the SNPs overlapping with TIAR/ELAVL1 binding sites have a PHRED score >10.

SUPPLEMENTARY FIGURES

Supp. Fig. 1. Comparison between predicted and observed RBP interactions with *SNCA* long 3' UTR. A) *cat*RAPID *omics* (black curve) and *cat*RAPID *Global Score* (red curve) efficiently identify RBP interactions revealed by protein-arrays. Comparing strong signal RBPs (top 50 and bottom 50 interactions ranked by signal to background ratio), we obtained and Area under the ROC curve of 0.78 for *cat*RAPID *omics* and 0.92 for *cat*RAPID *Global Score*. **B)** Correlation between *cat*RAPID *omics* scores and number of RBP binding sites reported in AURA (9, 10) (Pearson's correlation of 0.90; hyperbolic tangent with two fitting parameters used).

Supp. Fig. 2. Relative mRNA abundances of the three constructs carrying the sequence of *SNCA* 3'UTR S (575 nt), M (1074 nt) and L (2530 nt) at the 3' of luciferase coding sequence measured by qPCR. *p-value<0.05 calculated with Wilcoxon's test.

Supp. Fig. 3. RNA and protein expression levels upon depletion of TIAR and ELAVL1. A-B Quantitative real time PCR of SNCA, TIAR and ELAVL1 mRNA relative expression in HeLa control and KD cells using two different shRNAs for each protein. Three different housekeeping genes (ACTB, PPIB and RPS18) for normalization of gene expression are compared. C-D western blot analysis of SNCA, TIAR and ELAVL1 in control and KD conditions.

Supp. Fig. 4. RNA affinity purification in presence and absence of UV cross-linking. TIAR and ELAVL1 are co-purified with *in vitro* synthesized RNA of *SNCA* 3'UTR long and short in presence (+) or absence (-) of UV cross-linking proving that the interaction observed

is not due to a technical artifact of the cross-linking. Also in this condition ELAVL1 binds to *SNCA* 3'UTR long with higher avidity than *SNCA* 3'UTR short, while TIAR shows similar binding ability for both 3'UTRs.

Supp. Fig. 5. Fragments A, B and C: ELAVL1 and TIAR equilibrium dissociation constants.

Supp. Fig. 6. TIAR, ELAVL1 and α-synuclein protein expression in primary cultured fibroblasts from human skin biopsies. (A) α-synuclein TIAR and ELAVL1 relative protein level in primary fibroblasts of control individuals, idiopathic PD, LRRK2-associated PD and MSA patients measured by western blot. (B) and (C) Normalized average values represented in the boxplot show a significant downregulation of TIAR protein in PD and MSA patients with respect to healthy control group (∗p-value < 0.05, Wilcoxon's test). (D) and (E) Similar results were observed for TIAR protein when idiopathic PD and LRRK2-associated PD cases are considered as separate groups, while in the case of ELAVL1, a significant upregulation is measured in LRRK2-associated PD cases with respect to control individuals. (∗p-value < 0.05, Wilcoxon's test).

Supp. Fig. 7. Normalized *SNCA* expression associated to rs7912058 variant. Ranked normalized *SNCA* gene expression in human *hippocampus* of rs7912058-C homozygous ('Homo Ref), rs7912058-CG heterozygous (Het) and rs7912058-G homozygous (Homo Alt) individuals. Data retrieved from GTEx project. The minor allele of the leading single nucleotide polymorphism (SNP) rs7912058-G is associated with decreased expression of *SNCA*.

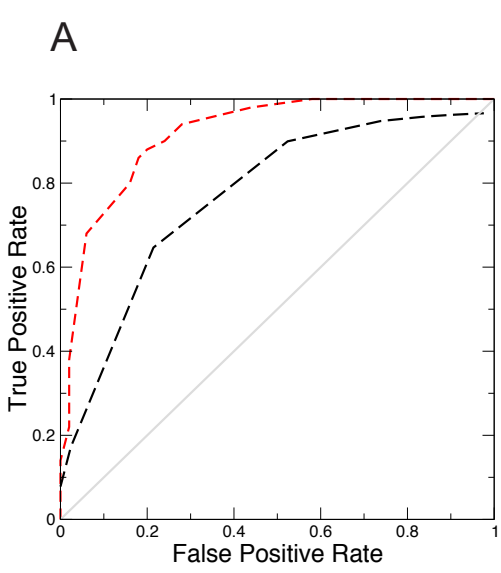
A
True Positive Rate
False Positive Rate
0
0.2
0.4
0.6
0.8
1

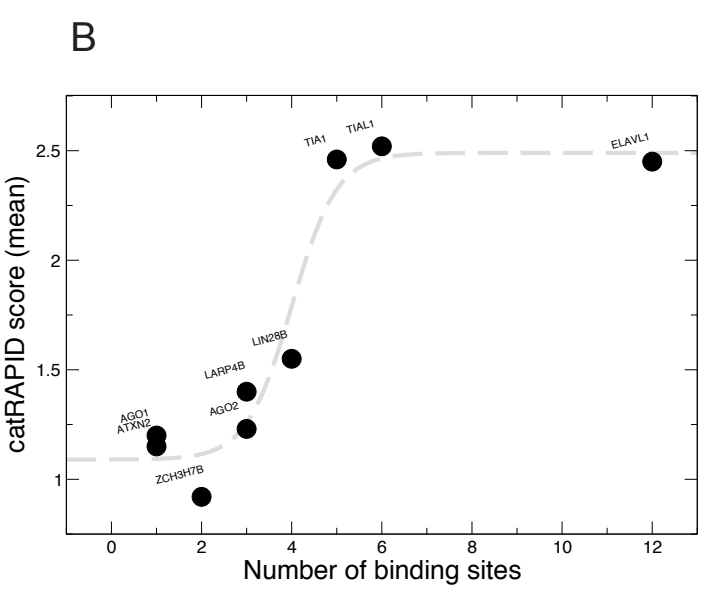
B
catRAPID score (mean)
Number of binding sites
TIA1
TIAL1
ELAVL1
LIN28B
LARP4B
AGO2
AGO1
ATXN2
ZCH3H7B
0
2
4
6
8
10
12
1
1.5
2
2.5

Supp. Fig. 1

Supp. Fig. 2

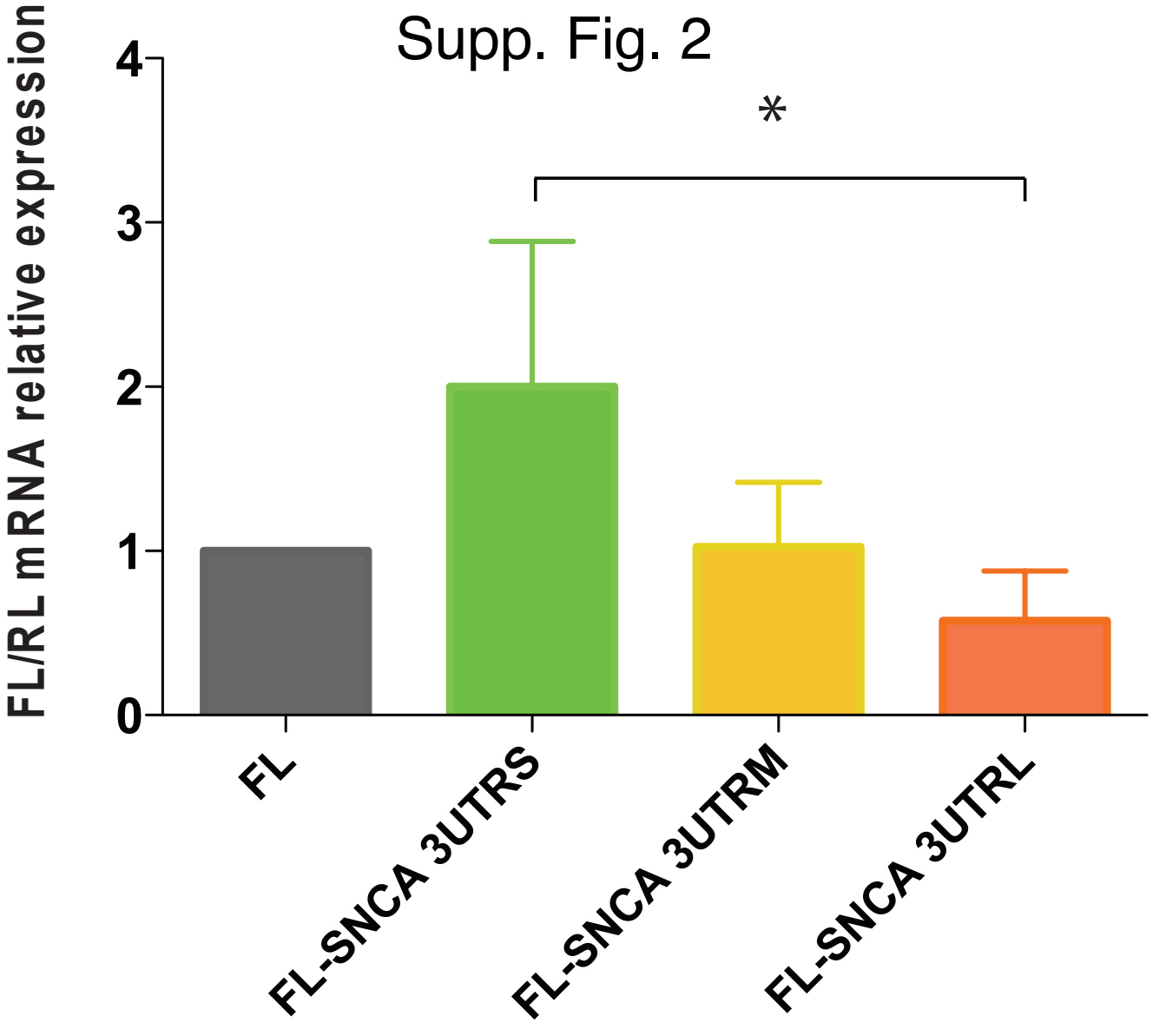
FL/RL mRNA relative expression
4
3
2
1
0
*
FL
FL-SNCA 3UTRS
FL-SNCA 3UTRM
FL-SNCA 3UTRL

Supp. Fig.3

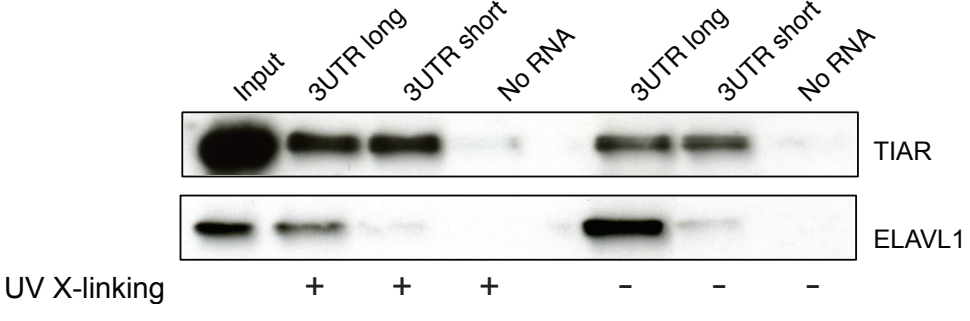
Input
3UTR long
3UTR short
No RNA
3UTR long
3UTR short
No RNA
TIAR
ELAVL1
UV X-linking
+
+
+
-
-
-

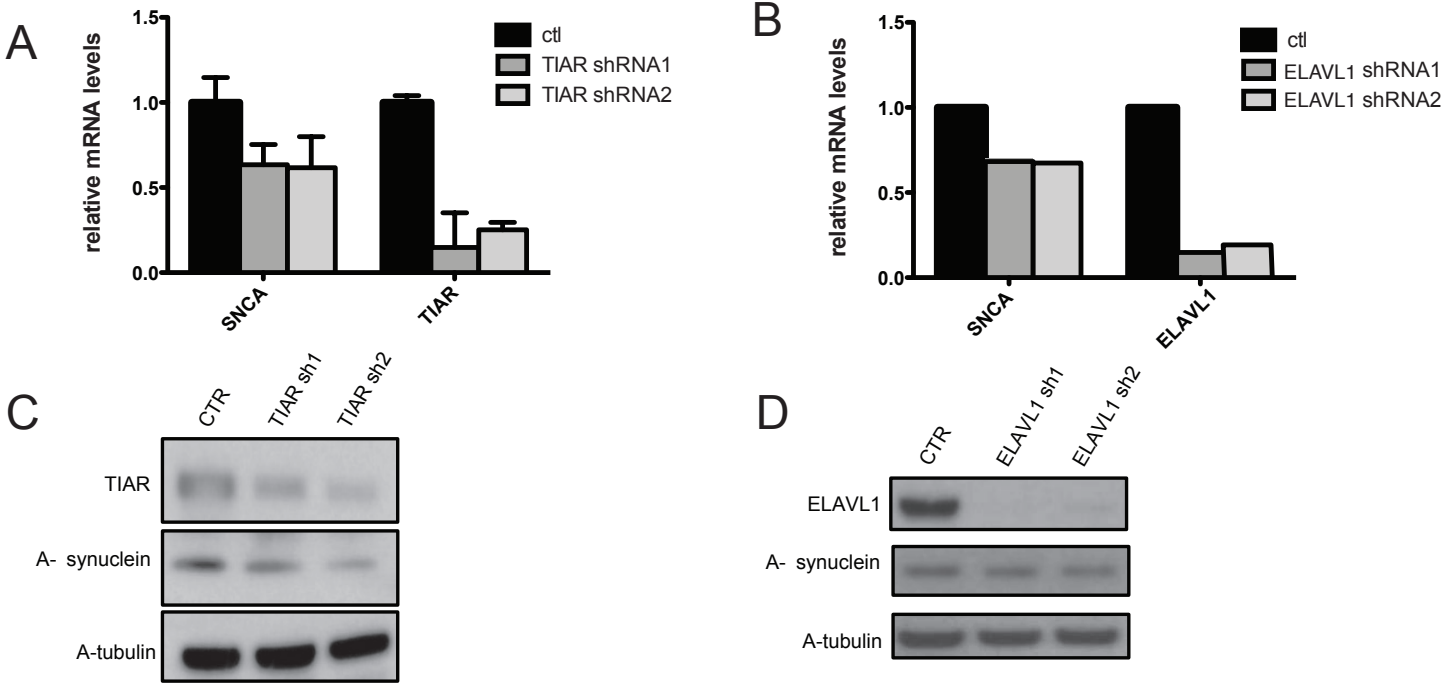
A
relative mRNA levels
1.5
1.0
0.5
0.0
ctl
TIAR shRNA1
TIAR shRNA2
SNCA
TIAR
B
relative mRNA levels
1.5
1.0
0.5
0.0
ctl
ELAVL1 shRNA1
ELAVL1 shRNA2
SNCA
ELAVL1
C
CTR
TIAR sh1
TIAR sh2
TIAR
A- synuclein
A-tubulin
D
CTR
ELAVL1 sh1
ELAVL1 sh2
ELAVL1
A- synuclein
A-tubulin

Supp. Fig. 4

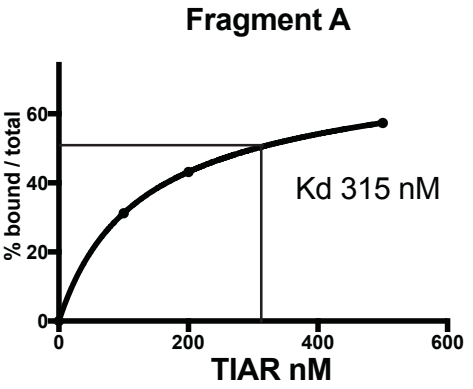
Fragment A
% bound / total
0
20
40
60
0
200
400
600
TIAR nM
Kd 315 nM

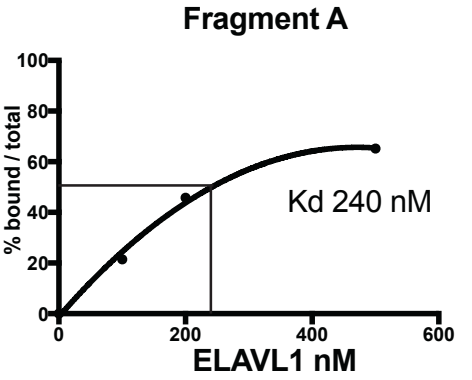
Fragment A
% bound / total
0
20
40
60
80
100
0
200
400
600
ELAVL1 nM
Kd 240 nM

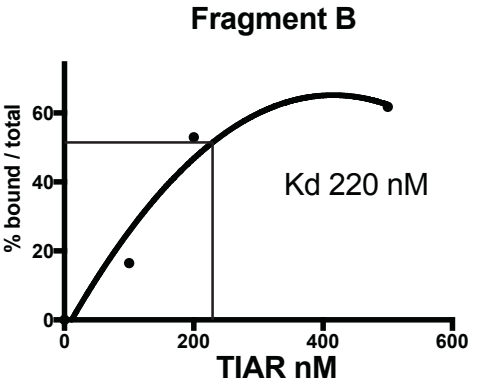
Fragment B
% bound / total
0
20
40
60
0
200
400
600
TIAR nM
Kd 220 nM

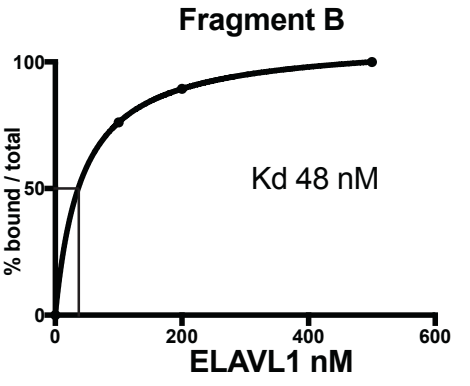
Fragment B
% bound / total
0
50
100
0
200
400
600
ELAVL1 nM
Kd 48 nM

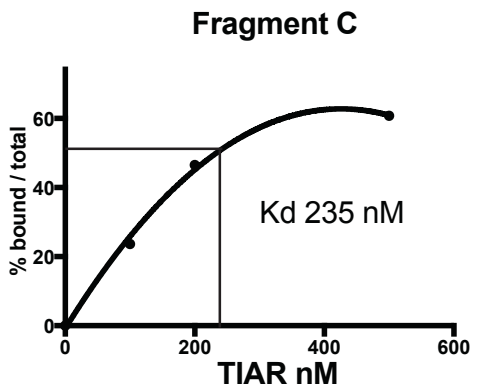
Fragment C
% bound / total
0
20
40
60
0
200
400
600
TIAR nM
Kd 235 nM

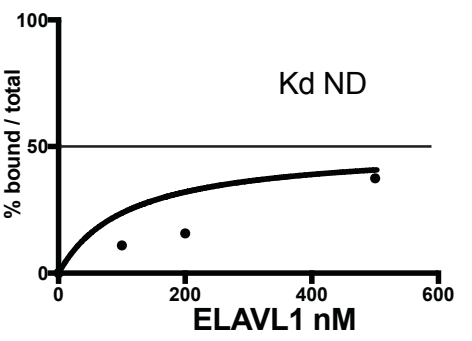
Fragment C
% bound / total
0
50
100
0
200
400
600
ELAVL1 nM
Kd ND

Supp. Fig. 5

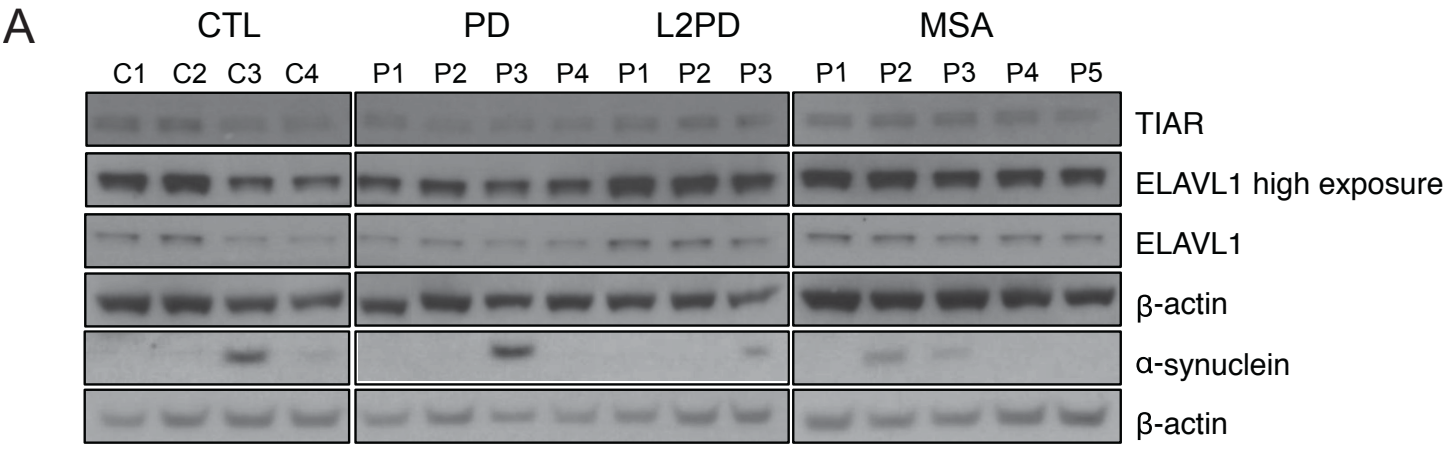
A
CTL
PD
L2PD
MSA
C1 C2 C3 C4
P1 P2 P3 P4
P1 P2 P3
P1 P2 P3 P4 P5
TIAR
ELAVL1 high exposure
ELAVL1
β-actin
α-synuclein
β-actin

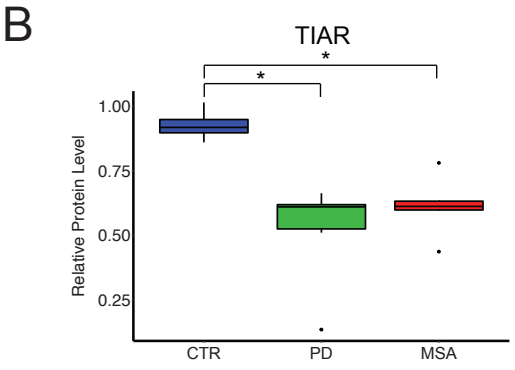
B
TIAR
Relative Protein Level
1.00
0.75
0.50
0.25
CTR
PD
MSA

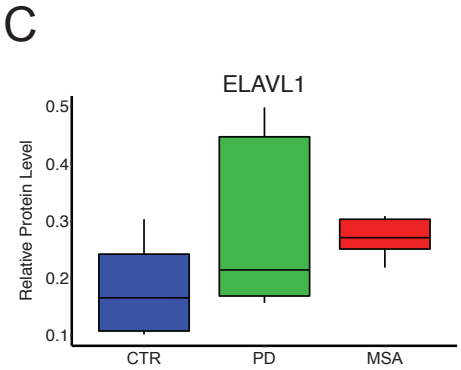
C
ELAVL1
Relative Protein Level
0.5
0.4
0.3
0.2
0.1
CTR
PD
MSA

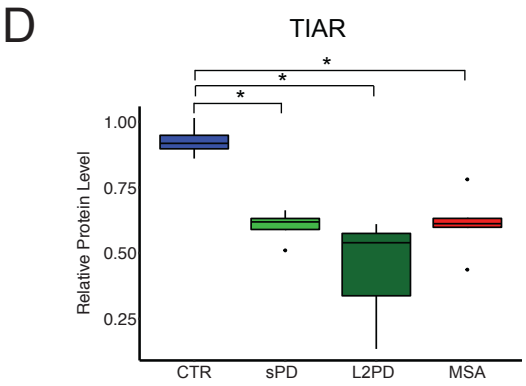
D
TIAR
Relative Protein Level
1.00
0.75
0.50
0.25
CTR
sPD
L2PD
MSA

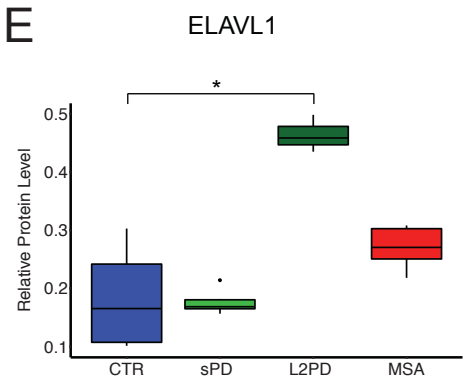
E
ELAVL1
Relative Protein Level
0.5
0.4
0.3
0.2
0.1
CTR
sPD
L2PD
MSA

Supp. Fig. 6

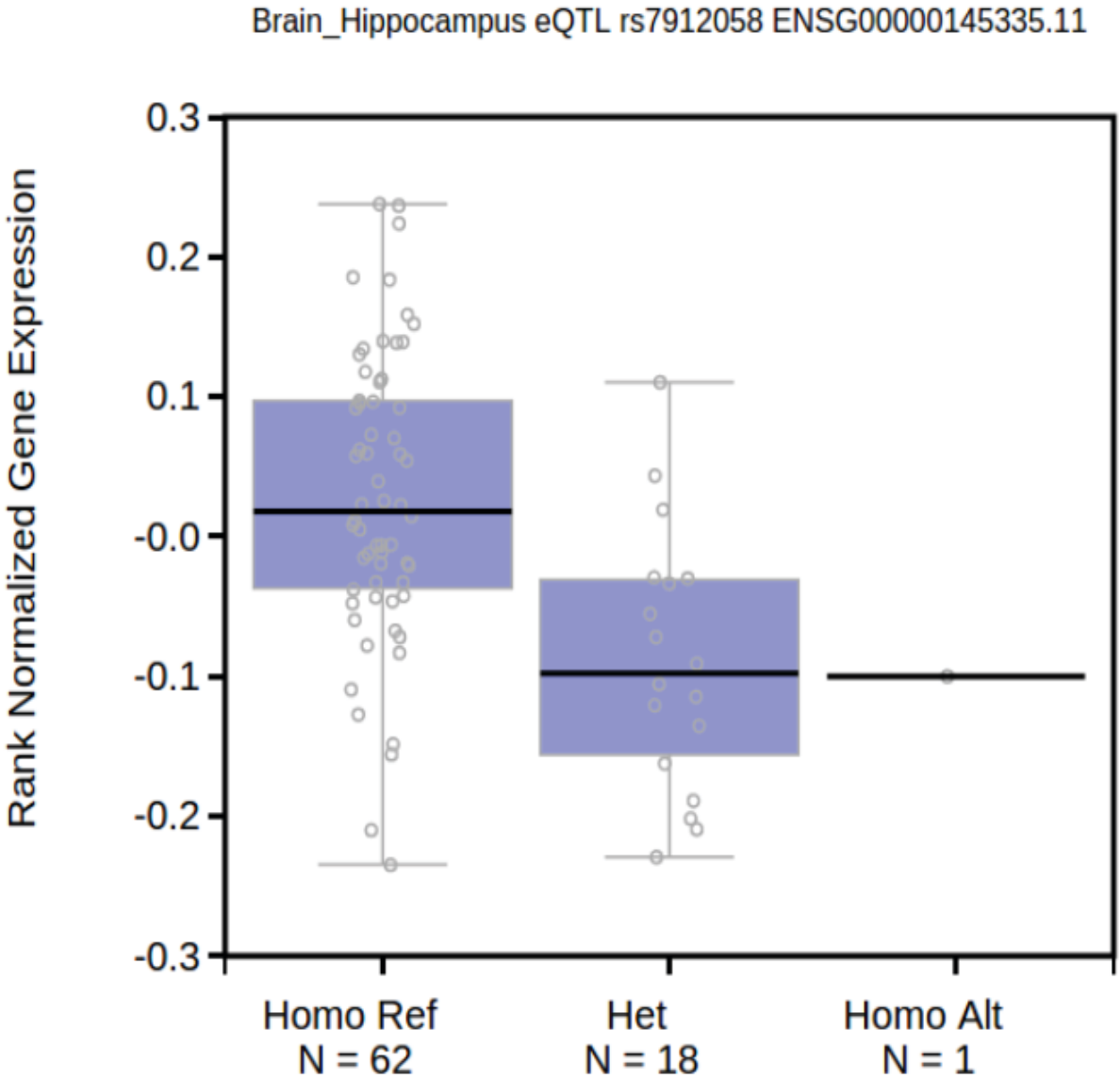
Brain_Hippocampus eQTL rs7912058 ENSG00000145335.11
Rank Normalized Gene Expression
0.3
0.2
0.1
-0.0
-0.1
-0.2
-0.3
Homo Ref
N = 62
Het
N = 18
Homo Alt
N = 1

Supp. Fig. 7

Group	Case N.	Diagnosis	Gender	Age	PMD (h:min)
Control	C1	Subcortical infarcts, leukoencephalopathy	Male	78	06:00
	C2	Minimal AgD I, mild gliosis, gastric cancer	Male	76	11:30
	C3	iLBD Braak 1, NFT I-II, SVD; lung cancer	Male	78	06:00
	C4	Right vertebral thrombosis+cerebellar and bulbar ictus, NFT III	Female	86	04:00
PD	P1	PD-D, Braak 5, ARP II B	Male	78	05:15
	P2	PD-D, Braak 4-5+ARP II A	Female	83	04:00
	P3	PD-D, Braak, 5, ARP II B	Male	71	05:00
	P4	PD-D, Braak 4, ARP III A, SVD	Female	90	05:30
	P5	PD-D vs DLB, Braak 5 + NFT II without plaques	Female	75	03:45
MSA	P1	Parkinsonian MSA, OPCA II, SND III, onset 50	Male	59	04:30
	P2	Parkinsonian MSA, OPCA II/III, SND III, onset na	Female	52	05:30
	P3	Parkinsonian MSA, OPCA II, SND III, onset 43	Female	51	05:45
	P4	Parkinsonian MSA, OPCA II, SND III, onset na	Female	69	06:00
	P5	Parkinsonian MSA, OPCA II, SND II-III, onset 52	Female	59	06:05

Supp. Table 1

Group	LRRK2 G2019S	Gender	Age at biopsy	AAO
control	negative	female	66	n.a.
control	negative	male	52	n.a.
control	negative	male	66	n.a.
control	negative	female	48	n.a.
sPD	negative	female	62	59
sPD	negative	male	54	48
sPD	negative	female	51	n.a.
sPD	negative	male	46	40
L2PD	positive	male	44	34
L2PD	positive	female	63	50
L2PD	positive	female	68	57
MSA-P	negative	female	62	57
MSA-P	negative	male	55	43
MSA-P	negative	male	72	66
MSA-P	negative	male	62	59
MSA-P	negative	female	59	57

Supp. Table 2

mirna	target	mirna_start	mirna_stop	rbp	rbp_start	rbp_stop	conservation	public_hela_avg	internal_hela_avg
hsa-miR-539	SNCA	276	297	ELAVL1	287	314	+	0.000	1.120
hsa-miR-126*	SNCA	587	607	TIAL1	593	595	-	2.340	0.820
hsa-miR-570	SNCA	306	328	ELAVL1	287	314	-	0.000	0.640
hsa-miR-1224-5p	SNCA	287	305	ELAVL1	287	314	-	0.159	4.030
hsa-miR-921	SNCA	283	308	ELAVL1	287	314	-	0.285	1.580
hsa-miR-1294	SNCA	285	306	ELAVL1	287	314	-	0.536	1.580
hsa-miR-3120	SNCA	302	323	ELAVL1	287	314	-	0.000	1.220
hsa-miR-3134	SNCA	572	594	TIAL1	593	595	-	0.000	1.220
hsa-miR-3174	SNCA	283	307	ELAVL1	287	314	-	1.557	1.220
hsa-miR-3065-5p	SNCA	298	319	ELAVL1	287	314	-	0.527	3.520
hsa-miR-4316	SNCA	290	306	ELAVL1	287	314	-	0.000	1.840

Supp. Table 3